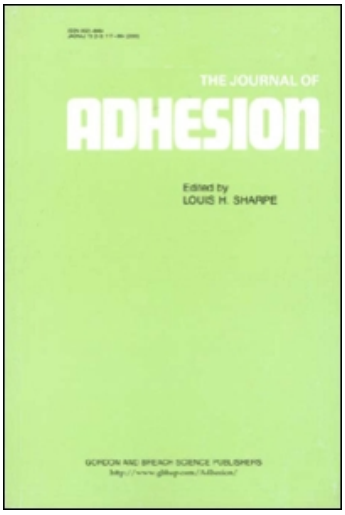

The Journal of Adhesion

Publication details, including instructions for authors and subscription information:
http://www.informaworld.com/smpp/title~content=t713453635

Adhesion of Plasticized Polyvinyl Butyral) to Glass

J. R. Huntsberger[a]
[a] Polymer Products Department, E. I. du Pont Nemours and Company, Inc. Experimental Station, Wilmington, Delaware, U.S.A.

To cite this Article Huntsberger, J. R.(1981) 'Adhesion of Plasticized Polyvinyl Butyral) to Glass', The Journal of Adhesion, 13: 2, 107 — 129
To link to this Article: DOI: 10.1080/00218468108073180
URL: http://dx.doi.org/10.1080/00218468108073180

J. Adhesion, 1981, Vol. 13, pp. 107–129
0021–8464/81/1302–0107 $06.50/0

Printed in Great Britain

Adhesion of Plasticized Poly(vinyl Butyral) to Glass

J. R. HUNTSBERGER

Polymer Products Department, E. I. du Pont Nemours and Company, Inc. Experimental Station, Wilmington, Delaware 19898, U.S.A.

(*Received January 26, 1981; in final form May 25, 1981*)

A study of safety glass provides a good example of the interplay among the many physical properties involved in "adhesion", and the relationship between adhesion and performance. This work demonstrates the value of applying known fundamentals to practical problems.

An idealized model of a windshield fracture event is described in terms of interactions among mechanical responses of the interlayer, the fracture characteristics of the glass and the high speed, low angle peel behavior.

Data on the surface energies of glass, poly(vinyl butyral) and water show that at thermodynamic equilibrium a stable system comprising glass, water and poly(vinyl butyral) phases, an aqueous phase must lie between the glass and PVB.

The potassium salts are shown to be effective because they are deliquescent and give solutions at equilibrium with the water in the PVB at water contents of $\sim 0.40\%$ or higher. The greater the amount of salt at the interface and the higher the water content of the sheeting during lamination, the thicker the interfacial layer and delamination occurs more readily. This relationship is quantified using a modified form of the Stefan equation.

Data on diffusion of water and salt are shown to be consistent with the amount of salt at the interface required for the observed performance ($\sim 3\,\text{mg KAc/m}^2$).

Data on electrical resistivity of the interface correlate with peel force and provide convincing support for the hypothesis.

INTRODUCTION

This work was aimed at understanding the performance of safety glass. Safety glass is made by laminating ~ 0.76 mm of plasticized poly(vinyl butyral) between two pieces of plate or float glass ~ 2.5 mm thick.

Safety glass today is expected to prevent serious injury by preventing the head from penetrating the windshield and to do so without fracturing the skull. This latter requirement has been met by diminishing the thickness of the glass. Penetration is prevented by absorbing the kinetic energy through stretching the tough interlayer.

The poly(vinyl butyral) sheeting must delaminate partially to allow consumption of large amounts of energy.

Best performance requires an optimum amount of delamination and consequently close control of adhesive performance.

One of the effective ways to control the adhesive performance is to incorporate $\sim 0.1\%$ of potassium acetate in the sheeting and control the water content closely during lamination.

Optimum performance requires a balance between mechanical responses and adhesion.

RESULTS AND DISCUSSION

Relationship between mechanical properties and performance

An idealized model of the fracture event relates performance to high rate tensile properties, the glass fracture pattern, and delamination at high rates and low peel angles.

This is described by Figures 1 to 6. Figure 1 shows the crack pattern, Figure

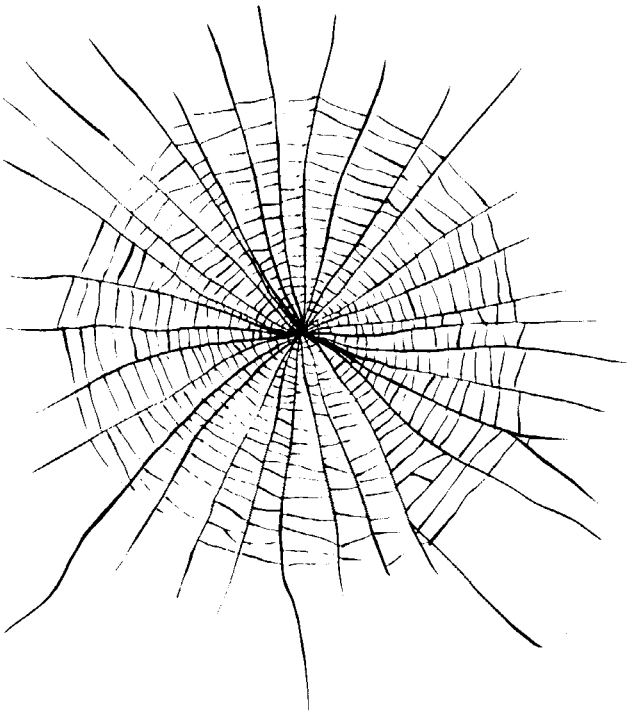

FIGURE 1 Crack pattern produced by impact of a 2.27 Kg ball.

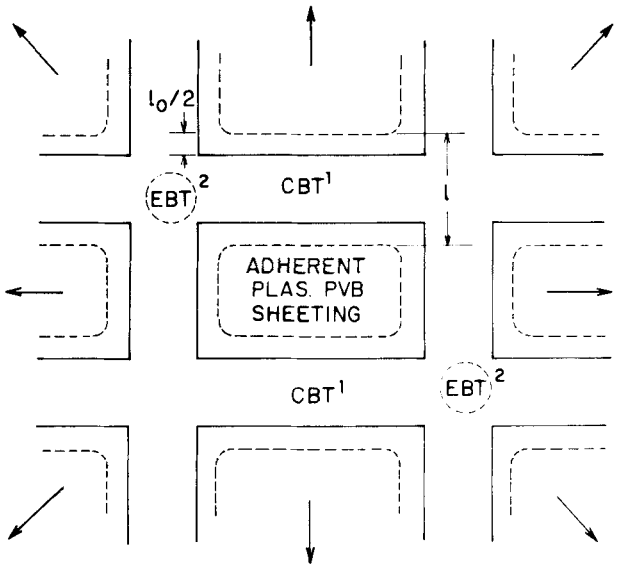

1 CBT = CONSTRAINED BIAXIAL TENSION
2 EBT = EQUAL BIAXIAL TENSION

FIGURE 2 Relative motion and resulting strain in PVB interlayer.

2 the relative motion of nine glass fragments and the associated strain in the sheeting. The strain is predominantly constrained biaxial tension with some equal biaxial tension at the juncture of four contiguous pieces.

Calculations are based on constrained biaxial tension using:

$$f = Gd_0\left(\lambda - \frac{1}{\lambda^3}\right) \tag{1}$$

where f = force per meter width (or per meter of crack length) in N/m, G = shear modulus in Pa, d_0 = original unstrained thickness in meters and $\lambda = l/l_0$ = extension ratio. Equation 1 is based on Treloar's treatment[1] of rubber elasticity.

The shear modulus, G, is rate dependent. Over the rates involved experimental data showed a fair approximation as given by the following empirical relation:

$$G \sim 1.60 \times 10^6 \log \dot{\varepsilon} + 5.25 \times 10^6. \tag{2}$$

Calculations for the impact behavior are based on $G = 0.9 \times 10^7$ Pa and elongation at break (e_b) in constrained elongation = $1.35\, l_0$.

Standard sheeting thickness is 0.76 mm and the force per meter width at fracture in constrained biaxial tension is 15.5 kN/m.

The work per meter of crack length consumed in stretching the sheeting to fracture is:

$$W = Gd_0 \int_{l_0}^{l_b} \left(\lambda - \frac{1}{\lambda^3}\right) dl \tag{3}$$

which on integration gives:

$$W = Gd_0 \left[\frac{l^2}{2l_0} + \frac{l_0^3}{2l^2} - l_0\right] \tag{4}$$

For the defined case this reduces to:

$$W = 12.65\, l_0 \text{ Joules/m of crack length (for } l_0 \text{ in mm).}$$

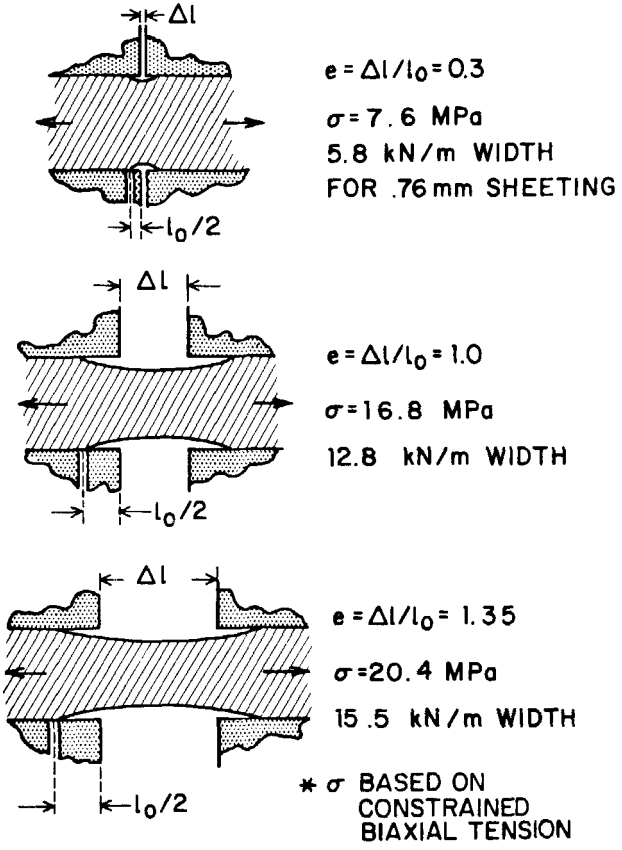

FIGURE 3 Schematic representation of delamination process.

Delamination of the sheeting and glass is a form of peeling which occurs by a process depicted in Figure 3.

The relationship between delamination and energy consumption is shown in Figure 4. Break heights diminish when delamination is too great. This is treated in the calculations by assuming increasing tearing initiated by notching of sheeting by sharp glass edges at delaminations greater than 1 mm. Notch initiated tearing leads to fracture at strains less than $1.35\,l_0$. Figure 5 shows how assumptions concerning the fracture mode influence calculated results. Figure 6 shows calculations for two different glass fracture patterns, one leading to a total crack length of 6.35 m, the other 3.81 m.

Increasing levels of peel strength lead to diminished delamination and consequently poorer performance which is measured by determining the mean drop height at which a 2.27 Kg steel ball just fails to penetrate. In Figure 6 we

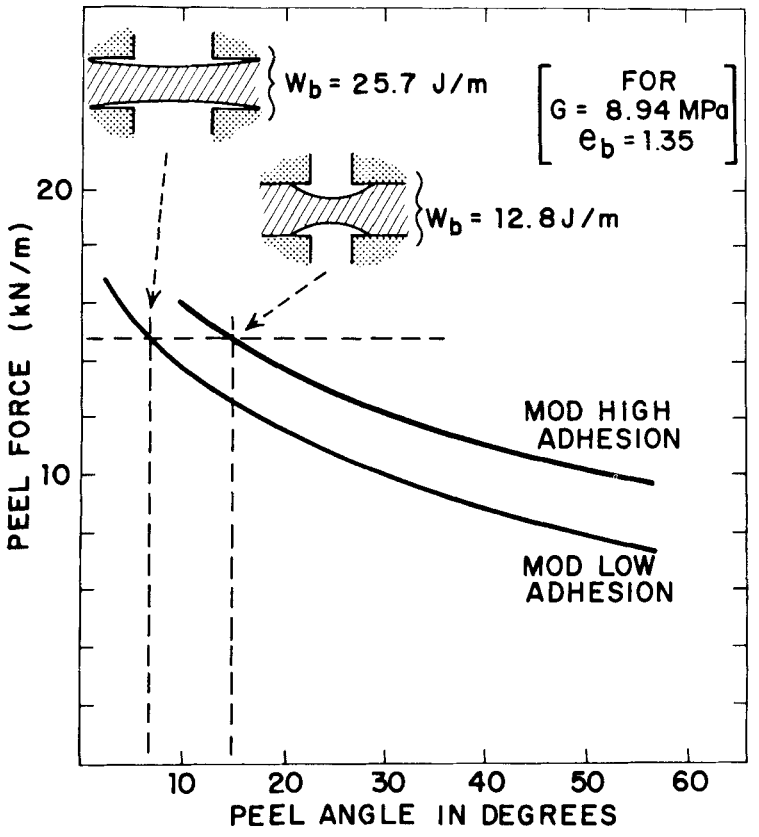

FIGURE 4 Relationship between adhesion, delamination, and energy consumption.

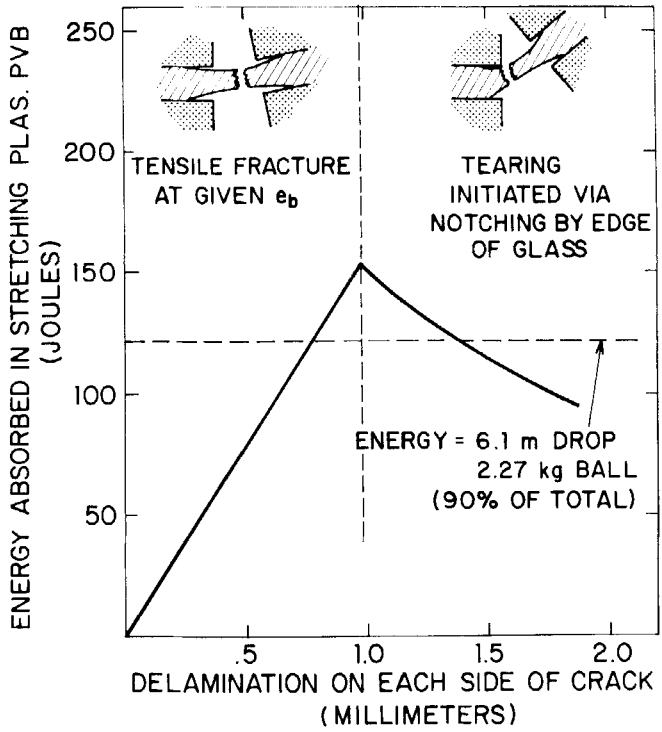

FIGURE 5 Model assumed for calculations.

see that when delamination falls below ~0.75 mm on each side of the crack, break height falls below 6.1 m. At 1 mm delamination the effective peel angle is ~10° and at 0.75 mm it is ~15° (corresponding to ~18–20% higher peel force if measured at 10°).

In Figures 5 and 6 the dashed line at 121 Joules represents 90% of the energy of a 2.27 Kg ball dropped 6.1 m. This is the approximate fraction consumed by stretching the sheeting. On the order of 10% is believed to be consumed in constrained layer damping. (This is based on unreported calculations by others.)

Adhesion and adhesive performance

Let us now examine adhesion and adhesive performance in detail.

Performance must be measured in a pertinent way. For this problem it is clear that this means high-rate, low-angle peel.

In order to carry out peel tests the samples used during this work were "half-

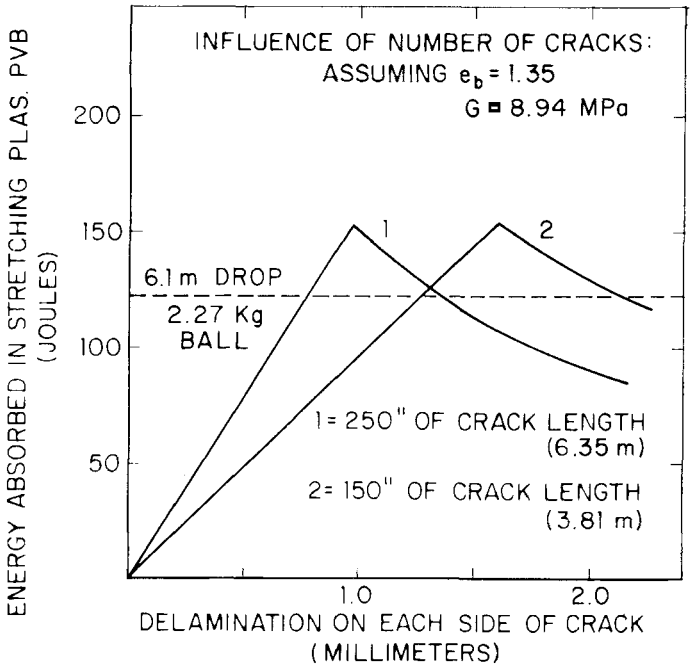

FIGURE 6 Energy absorption *vs.* delamination for 7.5 cm radius base and 62.7 mm penetration.

laminates" in which the poly(vinyl butyral) sheeting was laminated to a single piece of glass.

An apparatus was designed which would permit peeling at preselected angles from 10° to 90° at rates to 2 meters/second. A schematic representation of the action is shown in Figure 7. (The apparatus itself is omitted for clarity.) When the peeled sample is inextensible the peel angle θ is constant and equal to 2ϕ. This principle was used earlier by Packham.[2] Some characteristic data are shown in Figure 8.

Data to establish the angular dependence of peel force (Figure 9) were obtained using samples in which the elongation was prevented by laminating a strong, flexible but inextensible fabric to the poly(vinyl butyral) sheeting.

For convenience and to obviate changes in the sample most of the peel data were obtained at nominal peel angles which varied during the test as the sheeting stretched.

Since performance was known to be very sensitive to water content, initial studies were made to quantify this for the high rate peel data. Results are shown in Figure 10. Water content for these samples was measured conveniently and precisely by near IR spectroscopy using the ratio of

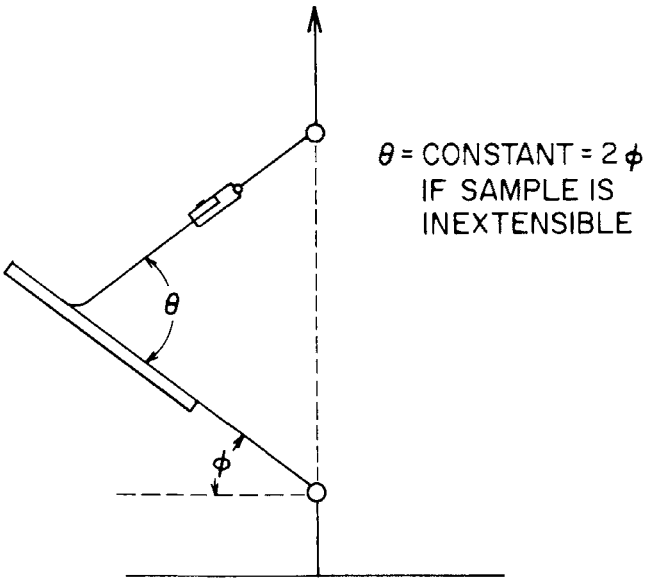

FIGURE 7 Schematic diagram for high speed variable (but constant) angle peel tester.

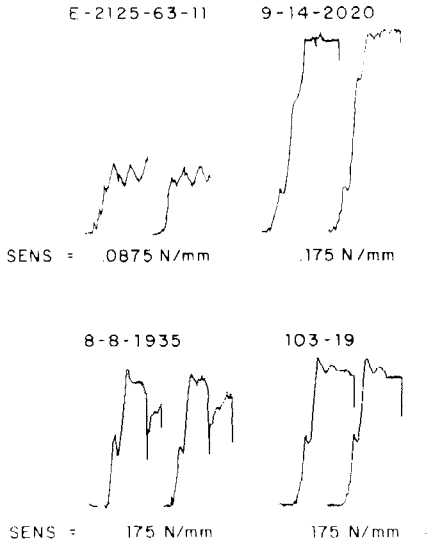

COEFFICIENT OF VARIATION FOR MEAN OF DUPLICATES IS ~ 2.0 TO 2.5 %

FIGURE 8 Examples of peel data.

absorptions at 1.93 μm and 1.70 μm. The water content is given by:

$$\%H_2O = 3.58(\text{abs. @ } 1.93\,\mu\text{m}/\text{abs. @ } 1.70\,\mu\text{m}) - 0.06$$

The influence of water was investigated further by examining the behavior of samples cycled between different levels of relative humidity. Five days were allowed at each exposure condition prior to measuring peel force. Results are given in Figure 11. Hysteresis is exhibited. Only after three cycles was the peel force at 50% R.H. similar to that of samples aged for long periods at 50% R.H. Subsequent cycling between 65% R.H. and 50% R.H. showed similar behavior. The long times involved suggest a very slow diffusion is involved.

These data along with some knowledge about the behavior of glass/adhesive bonds led to some questions about poly(vinyl butyral)/glass bonds.

The Owens and Wendt[3] method was used to estimate interfacial free energies of the various phases involved. Surface energies and fractional

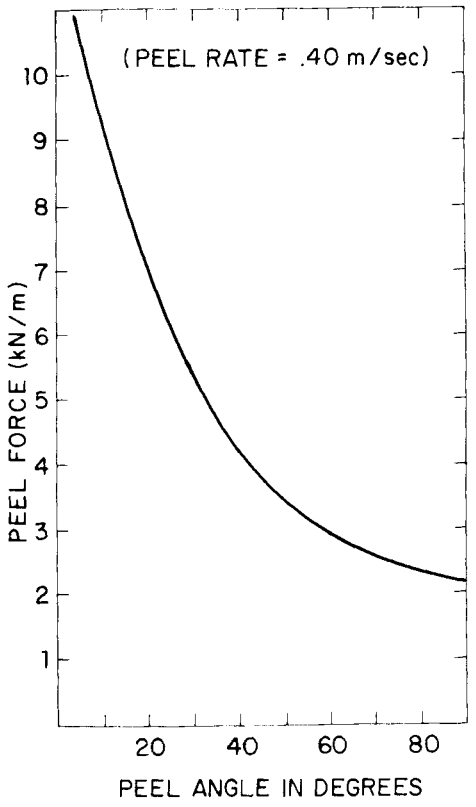

FIGURE 9 Peel force *vs.* peel angle for plasticized PVB sheeting (0.76 mm thick).

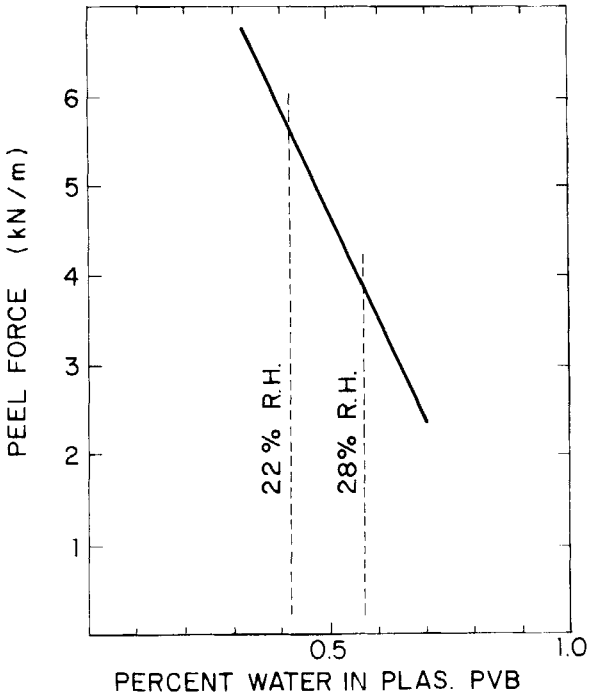

FIGURE 10 Peel force *vs.* water content of sheeting.

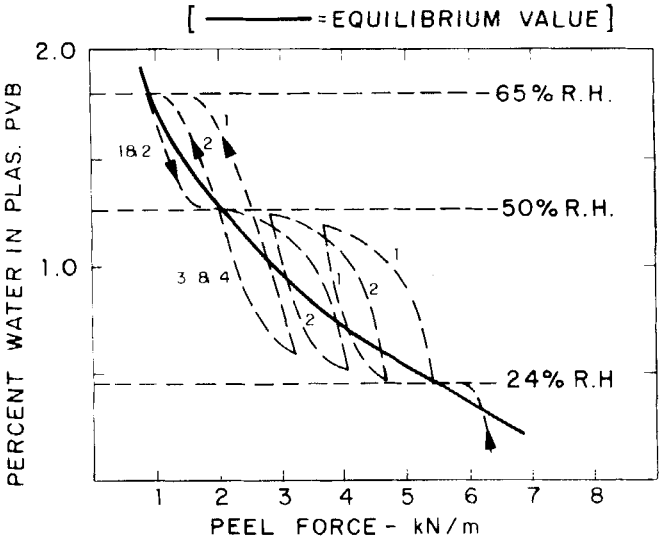

FIGURE 11 Influence of humidity cycling on peel force.

polarities[4] were determined from contact angle equilibria of water and methylene iodide. Pertinent data are given in Table I.

The reversible work of adhesion is given by:

$$W_{adh} = 2\phi(\gamma_1\gamma_2)^{1/2} \tag{5}$$

where γ_1 and γ_2 are the surface tensions of the individual phases in equilibrium with their own vapor pressures, and ϕ is Good's parameter which we will assume here makes Equation 5 exact.

The parameter ϕ can be approximated by:

$$\phi = (d_1d_2)^{1/2} + (p_1p_2)^{1/2} \tag{6}$$

and since:

$$\gamma_{12} = \gamma_1 + \gamma_2 - 2\phi(\gamma_1\gamma_2)^{1/2} \tag{7}$$

Using the data of Table I:
For:

Glass/plasticized PVB interactions	$\phi = 0.87$ and $\gamma_{12} = 134.5$ mN/m
Glass/water interactions	$\phi = 1.0$ and $\gamma_{12} = 62.4$ mN/m
Plasticized PVB/water interactions	$\phi = 0.89$ and $\gamma_{12} = 17.7$ mN/m

This shows that plasticized PVB/glass interfacial free energy is 54.4 mJ/m^2 greater than the combined glass/water and water/plasticized PVB interfacial energies.

We can conclude from this that the safety glass laminate interfacial regions comprise thin aqueous layers lying between the glass and sheeting.

It is known that on scrupulously clean glass, a monolayer of water exists at the interface even at low relative humidity. Glass surfaces of any nominal composition vary in production and also change with different cleaning methods. At 50% R.H. the thickness of water layers on glass cleaned with normal care may be from 1–4 nm thick.

On the basis of the thermodynamics and the experimental observation of

TABLE I

Surface energies and fractional polarities

Material	γ mN/m	γ^d mN/m	γ^p mN/m	d	p
Plasticized PVB	36	27	9	0.75	0.25
Glass	270	70	200	0.26	0.74
Water	72.8	21.8	51	0.30	0.70

d and p are fractional contribution of dispersion and polar interactions, respectively, to the surface tensions.

the influence of water on performance, the following working hypothesis was developed:

The cleaned, rinsed glass used in production of laminates contains small amounts of water soluble material whose kind and amount depend on the treatment. When plasticized PVB containing ~0.5% water and ~0.1% potassium salt is laminated to the glass, some water and salt are transported to the interface, and when the laminate cools it approaches an equilibrium in which the amount of interfacial water is controlled by the amount and nature of the salt. (For practical purposes the laminate can be treated as a closed system.) At equilibrium the activity of water must be constant throughout.

The activity of water is equal to the relative humidity at which the sheeting was equilibrated prior to lamination. The water content as a function of R.H. is shown in Figure 12. In practice sheeting contains ~0.5% water which means its activity is ~0.25. This means that salts which are effective in controlling adhesive performance must lead to equilibrium solutions stable at ~20–30% R.H.

The adhesive performance must be a function of the thickness of the interfacial aqueous layer.

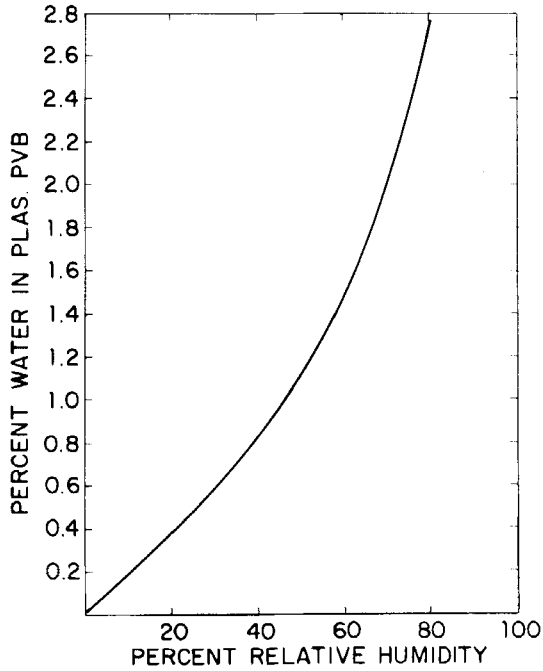

FIGURE 12 Equilibrium water content of plasticized PVB *vs.* relative humidity.

Subsequent work was aimed at testing the hypothesis and quantifying the behavior.

If performance is controlled by an aqueous layer which may be on the order of 5–10 nm thick it seemed possible that peel force may approximate behavior predicted by some form of the Stefan equation.[5]

$$F = \frac{3\pi}{4t}\eta\frac{R^4}{d^2} \tag{8}$$

This relates the force required to separate plates of radius R in time t when immersed in a liquid of viscosity η and initially separated by a distance d.

For plates separated by a fixed volume of liquid Healey[6] gives a modified form:

$$F = \frac{3}{8}\frac{\eta}{\pi t}\frac{V^2}{d^4} \tag{9}$$

where V is the volume of the liquid.

For a peeling event the effective volume in steady state peeling could be expressed as a product of the width of the strip, the thickness of the liquid layer and some effective length l_ε extending from the point of attachment through the deformed segment of the peeled strip ahead of the detached portion.

Making such a substitution for the volume in Eq. 9 and combining all constants into a single term K we get simply:

$$F = KU/d^2 \tag{10}$$

where the time has been changed to a steady state peel rate U.

Using $d = 1.5$ nm for the thickness of water at 50% R.H. for laminates made without potassium salts, and experimental data at a fixed nominal angle and rate for the force required to peel 0.76 mm additive-free sheeting equilibrated at 50% R.H. allows evaluating K in Eq. 10:

$$F = 2.76 \times 10^4\, U/d^2 \tag{11}$$

where d is in nm, and U in m/sec. F is in Newtons/meter.

Using Eq. 11 peel force was plotted as a function of aqueous layer thickess (Figure 13).

From Eq. 11 we predict that peel force should be a linear function of peel rate and should approach zero at very low rates. This was tested giving the data of Figure 14.

Potassium acetate and potassium formate were known to be effective adhesion control additives. It was also known that sodium acetate was ineffective. Handbook data were sufficient to show that both potassium acetate and potassium formate were extremely soluble and formed saturated solutions at equilibrium at $\sim$20% R.H. at 20°C. Sodium acetate on the other

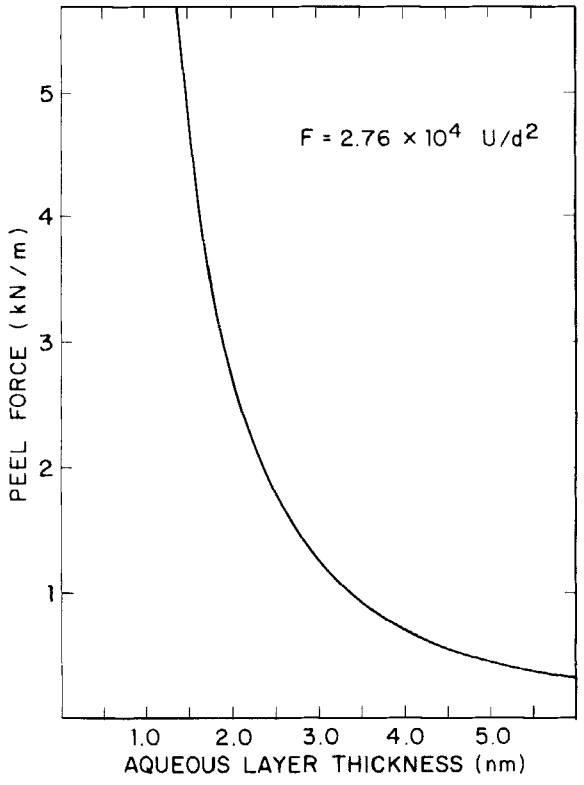

FIGURE 13 Peel force *vs.* aqueous layer thickness (based on modified Stefan equation).

hand forms saturated solutions (at 20°C) at 76% R.H. The effective salts meet the requirements of the hypothesis. The ineffective one does not. Cesium formate is also delequescent and was found effective in controlling adhesion when used to confirm or disprove the hypothesis.

This concept was pursued by measuring equilibrium salt concentrations for several salts equilibrated at 25, 50, and 81% R.H. Data are given in Table II:

How much potassium salt at the interface is required to diminish peel force was established through the following experiments.

Very thin PVB films ranging from 100–200 nm thick and containing 2 to 10% potassium acetate or potassium formate were coated on glass from dilute alcohol solutions. Laminates were made using 0.76 mm sheeting containing no additives and peel force was measured along with control samples with no thin films. These data showed that peel force diminished significantly when ~5 to 10 mg/m^2 of salt was within 200 nm of the interface.

Thin films of sheeting containing ~0.1% potassium salt were cast on glass

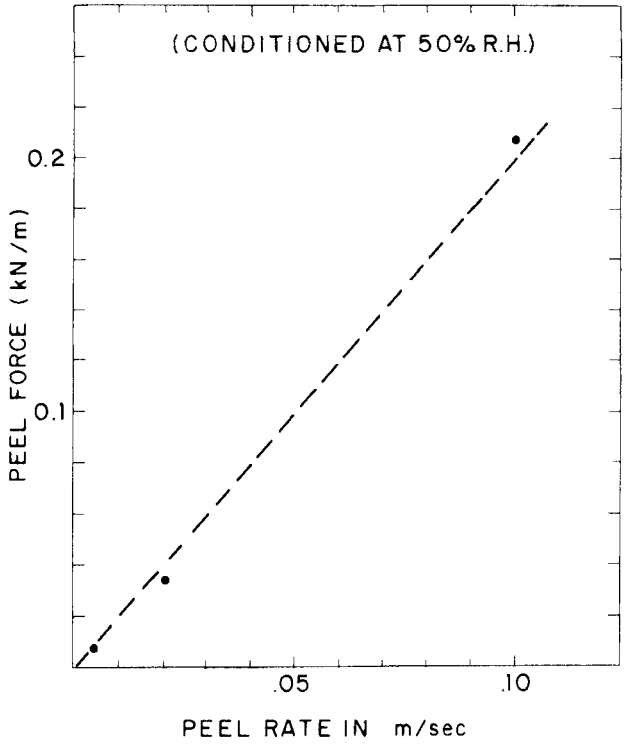

FIGURE 14 Peel force *vs.* peel rate at low rates.

giving films from a few hundred nm to $\sim 25\,\mu$m thick. Laminates made with these showed that peel force diminished when films containing 0.1% potassium acetate were $\geq 10\,\mu$m. This is $\sim 10\,\text{mg/m}^2$ within $10\,\mu$m from the interface.

A third kind of experiment consisted of depositing thin films of additive-free sheeting on the glass and preparing laminates with 0.76 mm sheeting containing 0.1% potassium acetate. Tests with these samples showed that $25\,\mu$m of additive-free sheeting was enough to prevent the salt from the 0.76 mm sheeting from diminishing peel force.

Taken together these experiments showed that adhesive performance is determined by the salt content and its distribution in a 20–25 μm layer near the sheeting surface with the concentration nearest the interface playing the major role.

Examination of the behavior of potassium salts in dry sheeting showed that the salts are not soluble in the plasticized poly(vinyl butyral). This means we can use the data on the volume concentration of water as a function of R.H. and the established data (Figure 12) on water content of sheeting as a function

TABLE II

Equilibrium salt concentrations at several relative humidities (as volume fractions):

Salt	25% R.H. Vol. fract. H_2O	Activity coeff. H_2O
K acetate	0.45	0.35
K formate	0.39	0.41
Cs formate	0.25	0.38
Salt	**50% R.H. Vol. fract. H_2O**	**Activity coeff. H_2O**
K acetate	0.57	0.63
K formate	0.54	0.68
Cs formate	0.42	0.62
Salt	**81% R.H. Vol. fract. H_2O**	**Activity coeff. H_2O**
K acetate	0.80	0.88
K formate	0.80	0.89
Cs formate	0.64	0.88

of R.H. to determine the thickness of water in the interfacial layer as a function of the water content of the sheeting. This is shown in Figure 15.

These data provide a basis for comparing the influence of various deliquescent salts on adhesive performance by assuming fixed amounts of salt at the interface. Comparisons are given in Table III:

Since we know that the approximate amount of interfacial salt is ~ 1 to $5\,mg/m^2$, and from the modified Stefan equation (Eq. 11) we know the peel force as a function of the thickness of the aqueous layer, plots of peel force *vs.* water content of the sheeting can be made for various amounts of interfacial salt. These are given as Figure 16.

Agreement between these calculated values and experimental data is very good if the actual amount of interfacial salt is ~ 1.5 to $2.0\,mg/m^2$.

The hysteresis in humidity cycling suggests that the amount of interfacial salt may increase slightly on exposure to high R.H. It would not be unreasonable to expect a system with $1.5\,mg/m^2$ at the interface at 25% R.H. to increase to $2\,mg/m^2$ at 45–50% R.H.

The working hypothesis requires diffusion of water and salt to the interface to form the thin aqueous layer.

The experiments on humidity cycling and the thin film experiments provided strong evidence for this and also indicated relatively slow diffusion.

Diffusion of water through plasticized poly(vinyl butyral) was measured giving a diffusion coefficient $D = 0.98 \times 10^{-11}\,m^2\,sec^{-1}$.

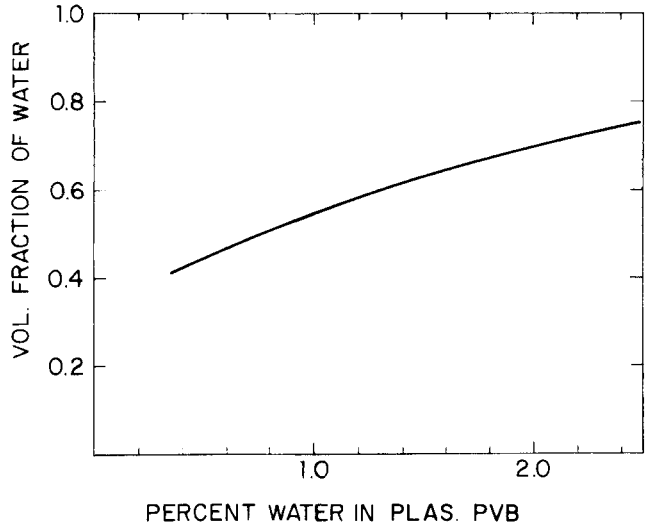

FIGURE 15 Volume fraction of water in the interfacial layer *vs.* percent water in the plasticized PVB sheeting.

Measuring D for potassium acetate was difficult. Data were not satisfactory but did show very clearly, however, that diffusion of salt is very slow. This supports the concept that the salts are virtually insoluble and dissolve only in the water present in the sheeting.

TABLE III

Thickness of interfacial aqueous layers for various deliquescent salts at fixed salt content

Salt	Thickness of aqueous layer in nm (for 2.5 mg salt/m^2)	(for 2.5 × 10^{-5} eq. salt/m^2)
	25% R.H.	
K acetate	2.55	2.5
K formate	2.15	1.8
Cs formate	2.15	3.85
	50% R.H.	
K acetate	3.3	3.2
K formate	2.85	2.4
Cs formate	2.7	4.8
	81% R.H.	
K acetate	7.0	6.85
K formate	6.6	5.55
Cs formate	4.3	7.6

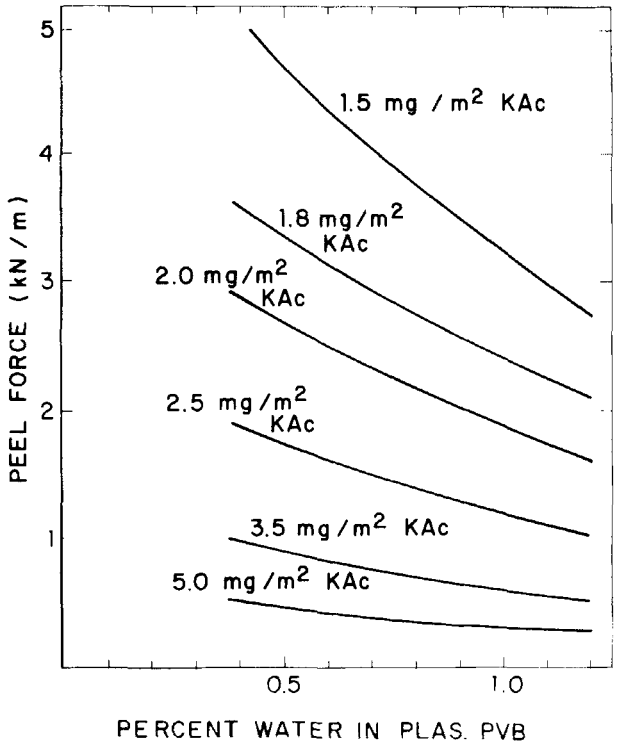

FIGURE 16 Peel force *vs.* water content (at various levels of KAc at the interface).

Using this concept an effective diffusion coefficient was calculated using:

$$D_A = \frac{KT}{6\pi} \frac{1}{R_A \eta_B} \tag{12}$$

where D_A is the diffusion coefficient of potassium acetate in water, R_A is an estimated radius for the hydrated K^+ ion plus the acetate ion, and η_B is the viscosity of the water. This gives $D_A \sim 2.7 \times 10^{-10}\,m^2\,sec^{-1}$.

For potassium acetate associated only with the water in the sheeting, the effective path length for diffusion is a function of the volume fraction of water in the sheeting. An effective diffusion coefficient for potassium acetate in the sheeting can be calculated using:[7]

$$D = D_A[1 + \phi_B/1 - \phi_B]^{-2} \tag{13}$$

where ϕ_B is the volume fraction of the sheeting. A plot of D *vs.* water content is given in Figure 17.

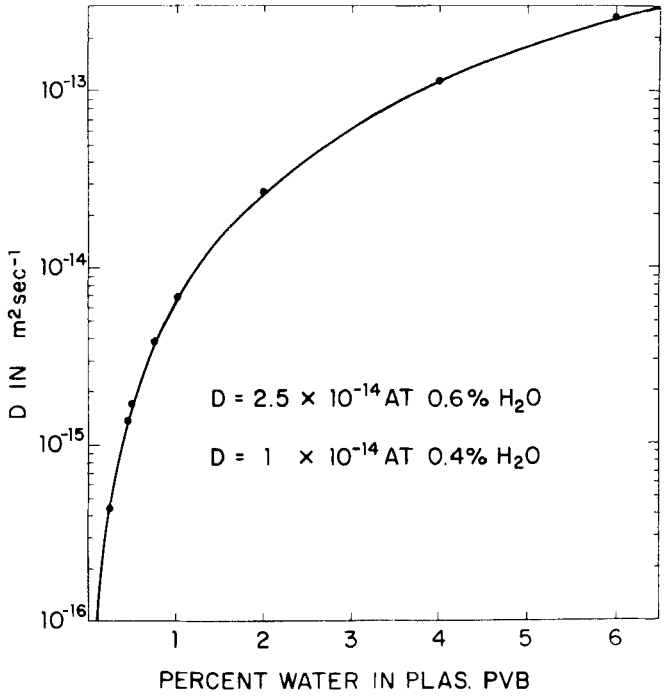

FIGURE 17 Effective diffusion coefficient for KAc in plasticized PVB *vs.* water content.

The best experimental data obtained using atomic absorption spectroscopy to measure potassium gave values for $D \sim 0.4 \times 10^{-14}\,m^2\,sec^{-1}$. The great disparity between diffusion of water and salt suggests that salt is transported mainly by association with migrating water. The value $D = 0.4 \times 10^{-14}$ for potassium acetate does, however, permit diffusion of $10\,mg/m^2$ across $10\,\mu m$ during lamination.

Further verification of low diffusivity of potassium salts was provided by spreading 5× the normal amount of salt over the sheet/air interface of additive-free sheeting previously laminated to glass. After two months the performance did not change.

Since the performance is controlled largely by a thin ($\sim 10\,\mu m$) layer near the surface, it seemed appropriate to try to quantify the influence of changes caused by non-steady state diffusion during short exposure times to various ambient conditions prior to lamination.

Unsteady state diffusion of water in sheeting is given by:[8]

$$\frac{x - x_0}{x_1 - x_0} = 1 - \text{erf}\,\frac{z}{(4Dt)^{1/2}} \tag{14}$$

where x_0 is the initial uniform concentration of water, x_1 is the concentration at the surface in equilibrium with the ambient R.H., and x is the concentration at a distance z from the interface. t is the time in seconds and D is the diffusion coefficient of water.

The amount of water absorbed in time t is:

$$\text{Amt } H_2O \text{ abs in } t \text{ sec} = 2\frac{(D)^{1/2}}{\pi}(x - x_0)t^{1/2} \tag{15}$$

For short exposures (in which penetration distance $\delta_t <$ half the sheeting thickness):

$$\delta_t = 4(Dt)^{1/2} \tag{16}$$

Using these the consequences of changes in exposure conditions can be calculated. This is shown in Table IV for penetration distance, amount of water absorbed, the average water concentration, and the mean concentration within 20 μm of the surface given for sheeting originally containing 0.45% water and exposed at $t = 0$ to 50% R.H.

These relatively large changes provide an adequate explanation for differences in performance associated with different handling methods even though the average water content changes little.

The influence of changes in humidity has a counterpart in changes brought about by exposing sheeting whose temperature is different from that of the ambient.

The steady state moisture content of sheeting held at temperatures different from that of the 23.5°C fixed R.H. circulating ambient air is shown in Figure 18.

It is evident that cold sheeting would absorb water and water would diffuse out of warm sheeting. It is difficult to predict the consequences of these changes on the laminated interface since there is very likely some transport of salt in the direction of the water movement.

The reality of such influences can be demonstrated by the behavior of sheeting conditioned by long time storage at 23°C and 28% R.H. When

TABLE IV

Influence of time at 50% R.H. on water content of sheeting initially containing 0.45% water

Time	δ, μm	mg H_2O abs/m^2	Av. % H_2O	Av. % H_2O within 20 μm of surface
30 sec	69	176	0.47	0.99
60 sec	98	248	0.48	1.11
300 sec	219	554	0.52	1.22

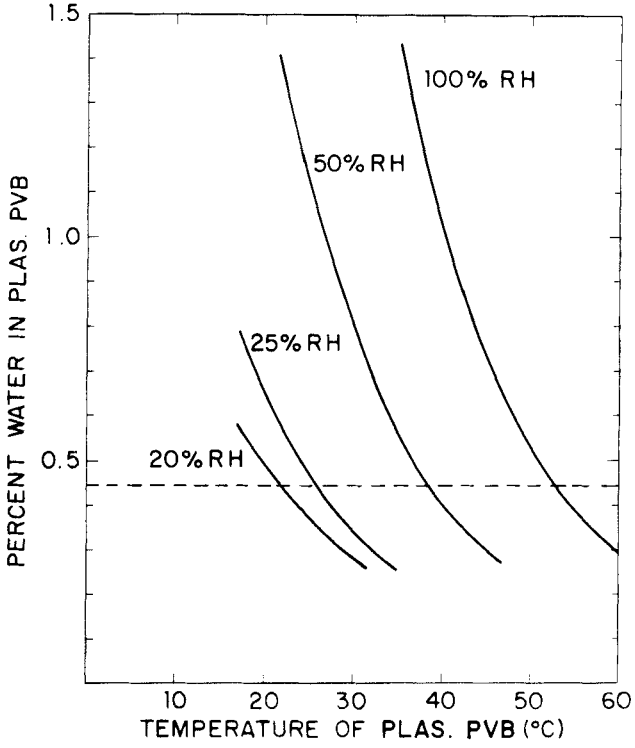

FIGURE 18 Water in plasticized PVB held at various temperatures at ambient 235°C and various R.H.

exposed for short periods to different conditions immediately prior to lamination (Table V).

If the interfacial region of these laminates contains the proposed aqueous layer, differences in the resistivity of the interface should be found at different water contents. Surface resistivities were measured by vapor depositing

TABLE V

Influence of short exposures to different conditions on behavior of sheeting

Exposure prior to lamination	% H_2O after lamination	Peel force (kN/m)
10 min @ 60% R.H.	0.66	2.17
10 min @ 60% R.H. followed by 10 min @ 35°C in 60% R.H. 23°C ambient	0.64	3.15

TABLE VI

Resistivities at 25% and 50% R.H.

Sample	Volume resistivity (ohm-meters) 25% R.H.	50% R.H.
Additive free sheeting	0.5×10^{15}	1.1×10^{14}
Sheeting with 0.1% KAc	0.2×10^{15}	0.3×10^{14}
Sample	**Surface or interfacial resistivity (ohms) 25% R.H.**	**50% R.H.**
Glass	2.1×10^{13}	5.5×10^{11}
Additive free sheeting	2.6×10^{13}	1.6×10^{12}
Sheeting with 0.1% KAc	4.6×10^{12}	3.5×10^{11}
Glass/additive free sheeting	1.6×10^{12}	1.2×10^{11}
Glass/sheeting with 0.1% KAc	1.9×10^{11}	1.1×10^{9}

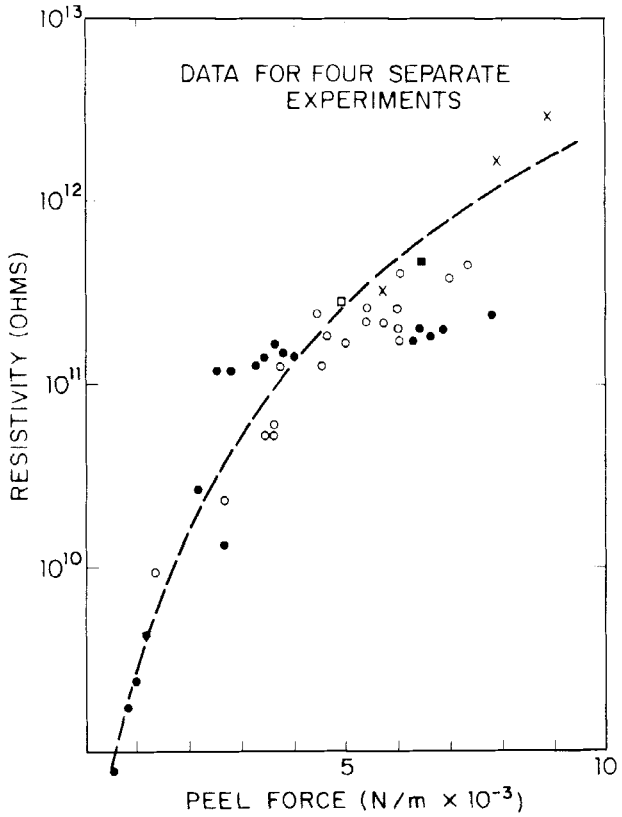

FIGURE 19 Relationship between resistivity of the interfacial layer and peel force.

electrodes on the glass surfaces prior to laminating. Resistivities were measured using a Keithly 610A electrometer. Data for a number of samples containing different amounts of salt and water are given in Table VI.

These data show the expected low interfacial resistivity and the marked decrease with increasing R.H. shown by glass/sheeting with 0.1% KAc. The data show that the interfacial resistivity is too low to be explained on the basis of a parallel combination of the individual surface resistivities and support the hypothesis.

These data suggested seeking a correlation between interfacial resistivity and peel force. Figure 19 shows this correlation.

CONCLUSIONS

No tests of the stated hypotheses were able to disprove them, and the efforts to quantify the mechanisms led to data and calculated values which were compatible and mutually supportive. This indicates an aqueous interfacial layer does in fact exist and controls the performance of sheeting employing potassium salts.

References

1. L. R. G. Treloar, *The Physics of Rubber Elasticity* (Oxford Press, 1949).
2. D. E. Packham in *Aspects of Adhesion* 6 D. J. Alner, Ed. (London University Press, London, 1970).
3. D. K. Owens and R. C. Wendt, *J. App. Polym. Sci.* **13,** 1741–1747 (1969).
4. J. L. Gardon, *Encyclopedia of Polymer Science and Technology*, Mark, Gaylor and Bikales, Eds. (Interscience, N.Y., 1965).
5. M. J. Stefan, *Sitzber. Akad. Wiss. Wien, Math. Naturw. Kl 11* **69,** 713 (1874).
6. A. Healey (in R. W. Griffiths), *Trans. Inst. Rubber Ind.* **1,** 334 (1926).
7. P. Mears, *Diffusion in Polymers*, Crank and Park, Eds. (Academic Press N.Y., 1968).
8. R. B. Bird, W. E. Stewart and E. N. Lightfoot, *Transport Phenomena* (Wiley, N.Y., 1960).